DEFLECTORS AS THE PERFORMANCE BOOSTER COMPONENT IN DESIGNING A SIDE-VENTILATED HEAT PUMP CABINET DRYER FOR VEGETABLES

by

Peter MECHA[a,b], Fang YALI[a], Emmanuel AWUAH[a], Joseph ODERO ALELE[a,b], Jiayu ZHANG[a], and Chen KUNJIE[a*]

[a] College of Engineering, Nanjing Agricultural University, Nanjing, China
[b] Faculty of Engineering and Technology, Egerton University, Egerton, Kenya

Original scientific paper
https://doi.org/10.2298/TSC230305130M

Unbalanced drying air and temperature distribution in a dryer is among the major cause of non-uniformity in moisture content of dried food. Thus, the distribution of air and temperature in corner-ended, corner-ended with deflector, curved-ended, and curved-ended with defectors were investigated. Velocities used were 2 m/s, 4 m/s, and 6 m/s while temperatures ranged from 40-60 °C. The design with lowest deviations in simulated and actual drying parameters was fabricated to dry mushrooms. Results showed that adding deflectors improved drying air and temperature distribution. The corner-ended with deflector dryer configuration was superior to other designs, with 6 m/s and 60 °C being optimal. A mass transfer simulation of the corner-ended with deflectors configuration had moisture evaporate from 1.00-0.11 in 2000 seconds. A comparison of moisture ratios in the two dryers gave $R^2 = 0.9965$, which was acceptable. Drying at 55-60 °C gave the best Lentinan content and rehydration ratio for mushrooms.

Key words: *twin-cabinet dryer, Lentinan, CFD simulation, rehydration ratio, mushroom drying, heat pump*

Introduction

Drying provides a preservation technique that minimizes food putrefaction in the agricultural sector. Dried products have the advantage of being used during the off-season period and eases transportation where production is limited [1]. Despite the merits mentioned, drying is an energy-intensive process in post-harvest processing unit operations taking up to 25% of the energy used in processing. Dry configuration is among the factors that affect a dryer's energy consumption and the quality of the drying process. Cabinet dryers are among the most favorite drying equipment. In an efficient cabinet dryer, uniform drying air temperature is desired and optimised based on the dried food type. Likewise, adequate and uniformly distributed air-flows for moisture transfer and minimum pressure differences at the air inlet and outlet is inescapable. Accordingly, cabinet dryers have proven more efficient due to possessing structural simplicity, cheap installation cost, and applicability to most environments. Despite the wide applications, cabinet dryers are limited in temperature and drying air distribution, causing a non-uniform drying rate which leads to dissimilarities in quality. The discrepancies are more prominent in cabinets arranged in series due to increased drying length and those positioned

* Corresponding author, e-mail: kunjiechen@njau.edu.cn

in parallel. The other cause of non-uniformity is that air is introduced under the bottom tray in most conventional cabinet dryers and moves up the trays.

Additionally, some cabinet dryers are made to introduce hot air from the source and exit at the furthest side of the tray. In either case, air at the next trays and the far end has high humidity, making hot air entry over-dried products while those at the exit are under-dried. The new version of twin cabinet dryers with separate side entrances and different configurations was investigated using CFD simulations to conquer the aforementioned problems. The best design was then fabricated and tested in this research. Rehydration ratio and lentinan content were then determined as quality parameters of the shiitake mushrooms.

Quality variations and reduction in drying energy are minimized using heat pump dryers designed to recover latent heat from moist air and uniformly distribute drying air and temperature in the chamber. This calls for dryer designs that ensure better distribution of drying parameters. Various researches have been done on improving temperature and air-flow inside dryers. For instance, studies done by Natalia *et al*. [2] showed that low local turbulence values could negatively affect the local mass transfer coefficients leading to non-uniform drying of turmeric. To reduce non-uniformity in cabinet dryers, Darabi *et al*. [3] designed dryers using two geometric configurations and separate air entrances for drying lemon fruits. The authors found that the new design with separate entrances had superior air velocity distribution than the existing designs. The influences of varying inlet air velocities are considered to improve the temperature uniformity inside the drying chamber, as suggested by Carrera *et al*. [4] in the design of chilli dryers. It was found from the work that slight differences in temperature and velocity distribution can be accepted since they cause minimal quality variations. Babu *et al*. [5] simulated four different drying chamber designs for thin layer drying of leafy vegetables. The best design was selected based on minimum pressure drop, maximum mass transfer rate with reduced drying time, the most uniform air temperature, and uniform air-flow distribution. They concluded that trays in the series improved the dryer's performance and hence more preferable [1] performed greenhouse dryer analysis with free and forced convection for the triangle, hemispherical and trapezoidal roof shapes. The researchers found that the trapezoidal roof shape greenhouse had a maximum temperature than the other shapes. As noted from most of these researches, there are inadequate attempts to simulate drying air and temperature distribution in twin cabinet dryers. More attention has been given to two single and series cabinet dryers. The proposed new designs are deemed to increase parametric uniformity by introducing curved ends, deflectors, and simultaneous entry and exit of drying air in the trays arranged vertically in each cabinet.

The CFD uses numerical processes to unravel non-linear PDE in fluid mechanics and heat transfer to resolve complex mechanisms governing food-processing systems [6] and drying processes [7]. The technique is better suited for the simulation process because it reduces experimentation time, correlates with experimental data, improves final dried products, optimizes the drying process, and optimizes energy consumption [2, 5]. The CFD gives a better assessment of air and temperature distributions in dryers, enabling design alterations before final fabrications [8, 9].

The novelty of this work is reflected in the simulation and experimentation of corner-ended, corner-ended with deflectors, curved-ended, and curved-ended with deflectors designs. The designs were assumed that could improve temperature and air distribution in the heat pump drying chamber. The best configuration was compared with the corner-ended configuration on which most common dryers are based. The CFD software ANSYS FLUENT tool was used to determine the best configuration with minimal deviations in experimental and simulated

drying conditions. Secondly, the impacts of temperature variations under constant velocity on Shiitake mushrooms' Lentinan content and rehydration ratio as quality outputs were determined using the preferred dryer configuration.

Materials and methods

Description of the designed heat pump cabinet dryer

The heat pump was designed at Nanjing Agricultural University, Agricultural Mechanization Department, while experimentations were performed at a Shiitake mushroom farm in Taizhou City, Jiangsu province, China. Shiitake mushrooms were used to investigate the drying behaviour of the designed heat pump. Heat pump design followed the steps described by Pal *et al*. [10] and Singh *et al*. [11]. The heat pump dryer system consisted of the heating system and the drying chamber part, fig. 1.

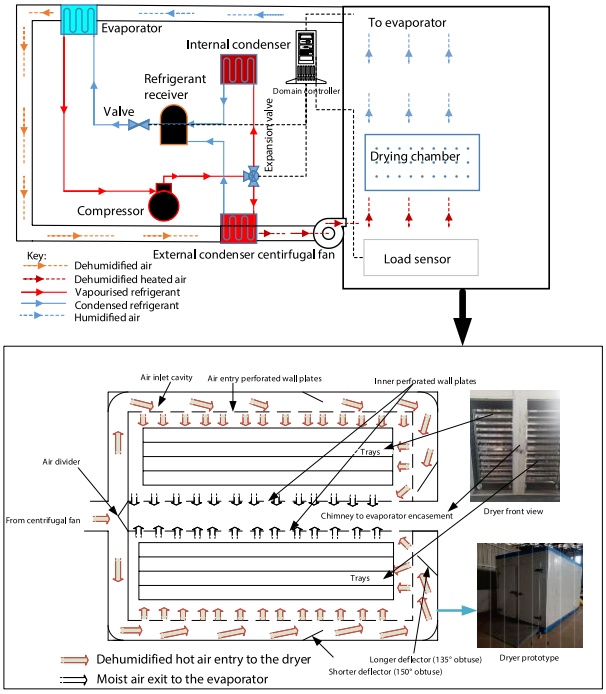

Figure 1. Heat pump dryer system

The heating part had an evaporator to dehumidify and recover latent energy from moist air. Dehumidified air was directed to the condenser for reheating. The reheated air was sucked and pushed into the drying chamber using a variable-speed centrifugal fan. The air inlet design was adjusted to allow air to enter all the trays concurrently from two sides and exit through a centrally placed chimney that directed moist air back to the evaporator. The dryer system was designed to hold 24 trays containing 20 kg of shiitake mushrooms. The dryer dimensions were a length of 2470 mm, 2210 mm wide, and 2300 mm high. Cabinet trays had uniformly distributed circular-shaped holes of ⌀20mm all over the surfaces. The research interest was determining the uniformity of drying air and temperature distribution in four proposed drying chamber configurations through CFD simulations and then fabricating the best design for drying experimentation. This was thought to optimize energy and quality in the twin heat

pump cabinet dryer. Drying air was let in from the sides to improve drying uniformity by not carrying a lot of moisture, as is the case when the distance moved to the exit is large.

Criteria of twin cabinet heat pump dryer configuration selection

To get the best geometric configuration, the curved-end configuration, cornered-end configuration, curved configuration with deflectors, and cornered-end configuration with deflectors, fig. 2, were assumed to guarantee uniformity in air and temperature distribution in the twin cabinet dryer. Geometrical parameters that influence air and temperature distribution patterns and the preferred dimensions for the twin cabinet dryer are shown in tab. 1. Temperature tested in the CFD ANSYS FLUENT tool were 40 °C, 50 °C, and 60 °C at velocities of 2 m/s, 4 m/s, and 6 m/s. Drying air was pushed by the centrifugal fan and made to flow into the twin cabinet dryers using an air divider at 170º and entered the drying area through side air cavities. Moisture-laden air exited through the chimney back to the evaporator for dehumidification for re-circulation.

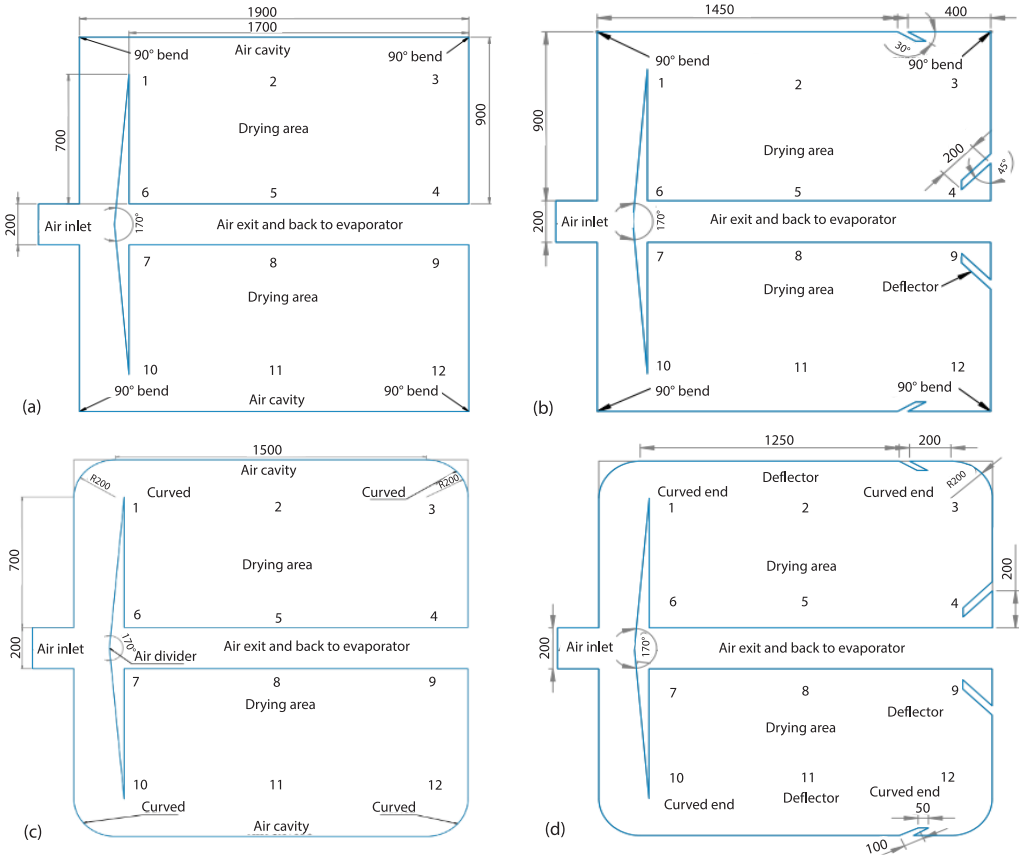

Figure 2. The 2-D proposed geometric configurations for the twin cabinet heat pump dryer; (a) corner-ended configuration, (b) corner-ended configuration with deflector, (c) curve-ended configuration, and (d) curve-ended configuration with deflector; *key: numbers at the drying area indicate velocity and temperature measuring sensor locations*

Table 1. Geometrical details of new twin cabinet dryer configurations

Geometrical parameter	Configuration type			
	Corner-ended	Corner-ended with deflectors	Curve-ended	Curve-ended with deflectors
Drying area	1700 mm x 700 mm	1700 mm × 700 mm	1700 mm × 700 mm	1700 mm × 700 mm
Air inlet size	200 mm × 200 mm	200 mm × 200 mm	200 mm × 200 mm	200 mm × 200 mm
Air cavity thickness	200 mm	200 mm	200 mm	200 mm
Chimney size	200 mm × 1700 mm	200 mm × 1700 mm	200 mm × 1700 mm	200 mm × 1700 mm
Curve radius	200 mm	200 mm	200 mm	200 mm
Longer deflector angle	45º	45º	45º	45º
Shorter deflector angle	30º	30º	30º	30º

The best configuration was selected based on uniformity velocity, temperature distribution, and minimal deviations in set and simulated conditions. After several trials, two sizes of deflectors and angles were used. The longer deflector (200 mm and at 45º) was placed 200 mm from the door, as the shorter deflector (100 mm) was established in the main air-flow cavity at 30º with the wall. The angles were placed against walls to deflect flowing air.

Basic governing equations for designing the twin-cabinet dryer

Three fundamental equations derived from mass and energy conservation principles are paramount in drying. Laminar flow was assumed due to the selected velocities having a lower magnitude. Steady 2-D was used for simulating the twin cabinet dryer due to reduced analysis complexities [12]. The *k-ε* model is the most preferred turbulent model with practical applications where *k* represents the exact transport equation given by eq. (1) while *ε* is the approximate physical value without precisely resembling its mathematical equivalence, [13]:

$$\frac{\partial}{\partial t}(\rho k)+\frac{\partial}{\partial x_i}(\rho k u_i)=\frac{\partial}{\partial x_j}\left[\left(\mu+\frac{\mu_t}{\sigma_k}\right)\frac{\partial k}{\partial x_j}\right]+G_k+G_b-\rho\varepsilon-Y_m+S_k \tag{1}$$

$$\frac{\partial}{\partial t}(\rho\varepsilon)+\frac{\partial}{\partial x_i}(\rho\varepsilon u_i)=\frac{\partial}{\partial x_j}\left[\left(\mu+\frac{\mu_t}{\sigma_\varepsilon}\right)\frac{\partial \varepsilon}{\partial x_j}\right]+C_{1\varepsilon}\frac{\varepsilon}{k}\left(G_k+C_{3\varepsilon}G_b\right)-C_{2\varepsilon}\rho\frac{\varepsilon^2}{k}+S_\varepsilon \tag{2}$$

Modelling convective drying in *k-ε* model in CFD ANSYS FLUENT tool is given:

$$\frac{\partial}{\partial t}(\rho E)+\frac{\partial}{\partial x_i}\left[u_i(\rho E+p)\right]=\frac{\partial}{\partial x_i}\left[\left(k+\frac{C_p\mu_t}{\mathrm{Pr}_t}\right)\frac{\partial T}{\partial x_i}+u_i\left(\tau_{ij}\right)_{\mathrm{eff}}\right]+S_h \tag{3}$$

A momentum source term was added to the standard fluid-flow to simulate the porous trays in the twin cabinet dryer and attain good turbulence with high temperatures in the mushroom trays:

$$S_i=-\left(\sum_{j=1}^{3}V_{xy}\mu\vartheta_j+\sum_{j=1}^{3}V_{xy}\rho\vartheta_{\mathrm{mag}}\vartheta_i\right) \tag{4}$$

where the first term represents the viscous loss term, while the second term is the inertial loss term. In drying, the moisture transfer equation in the dryer system is presented [5]:

$$\frac{\partial(\rho_a w)}{\partial t} + \nabla(\rho_a v w) = \nabla(\rho_a D_{\text{eff}} \nabla w) + S_w \tag{5}$$

The moisture source term, S_w, is expressed:

$$S_w = -(1-\varepsilon)\rho_m \frac{\partial w}{\partial t} \tag{6}$$

where ρ_m is the whwew being the particle density (determined as 875.5 kg/m^3) while ε was a porosity of 0.36 for shiitake mushrooms. The drying rate for shiitake mushrooms was given:

$$\frac{\partial w}{\partial t} = -k(W - W_e) \tag{7}$$

Combining eq. (6) and eq. (7), and as ε tends to 0, the moisture source term for mushrooms is simplified as shown in eq. (8). The sign of moisture source term depends on whether the product is gaining (–) or losing moisture (+). Since a drying product losses moisture, the sign is always positive (+):

$$S_w = \pm\rho_m k(W - W_e) \tag{8}$$

where k is the drying constant for shiitake mushrooms as obtained from Rhim *et al*. [14]:

$$k = 3.6 \cdot 10^{-3} \exp(0.0253T) \tag{9}$$

The instantaneous moisture content of shiitake mushrooms was calculated using:

$$W_{n+1} = W_n + \frac{\partial w}{\partial t}\Delta t \tag{10}$$

In analyzing heat transfer in the designed twin cabinet dryer, eq. (11) was applied:

$$\left(\rho_a \varepsilon c_a + \rho_b(1-\varepsilon)\left(c_g + c_w W + \frac{\partial H_w}{\partial T}\right)\right)\frac{\partial T}{\partial t} + c_a \nabla(\rho_a u T) = k_{\text{eff}} \nabla^2 T + S_h \tag{11}$$

The heat source term, S_h, for shiitake mushrooms was determined:

$$S_h = -h_s(1-\varepsilon)\rho_s \frac{\partial w}{\partial t} \tag{12}$$

Simulation process for the heat pump twin cabinet dryer

Since the equations suggested are non-linear, solving them using simple and analytical methods becomes complex and unrealistic. Consequently, the numerical finite volume method in ANSYS FLUENT (ANSYS 2020 version) was used to solve the equations numerically. A PC i7-8750H 4.41GHz having 16.0 GB installed RAM, 8$^{\text{th}}$ Generations, was used for simulations. The 2-D configurations were used to construct cell meshes. For improved accuracy and reduced error band, double precision in a segregated solver was used for simulation. The drying process under the twin dryers was also simulated as a steady-state since air-flow significantly affected the drying phase [12].

Specific boundary factors for the designed twin dryers were:

Inlet air: Velocity used was 2 m/s, 4 m/s, 6 m/s while the air temperature was 40 °C, 50 °C, and 60 °C. The direction of the air movement was normal from the side inlets.

Air exit: Gauge pressure = 0. The FLUENT software assumed pertinent details from the specific twin cabinet dryer configuration.

Porous media: Empiric parameters of the pressure drop relationship and bed porosity for the shiitake mushrooms were determined and set in ANSYS FLUENT.

Wall: Walls were assumed adiabatic with thermal conductivity with no slip. Specific heat and density of walls were taken from tab. 2. Experimentation was done in the early winter period at an ambient temperature of 10 ±1 °C.

Product used for drying: Shiitake mushrooms were used for experimentation since the project had an interest in designing a twin heat pump dryer more suitable for shiitake mushrooms.

Table 2. Properties of materials used for simulating twin cabinet dryer experiments

Material properties	Shiitake mushrooms	Cabinet tray (stainless steel)	Water	Drying air	Walls (polystyrene board)
Density [kgm^{-3}]	875.5	7990	1000	1.215	950
Specific heat [Jkg^{-1}K^{-1}]	3.935	0.5	4.182	1.005	1400
Conductivity [Wm^{-1}K^{-1}]	0.4398	45	0.6	0.025	0.48
Viscosity [kgm^{-1}s^{-1}]	–	–	0.001003	0.000011	–
Porosity	0.36	–	–	–	–

The number of nodes and element cells at mesh size of 0.02 m for each configuration is shown in tab. 3.

Table 3. Number of cells for the selected configurations

Chamber configuration	Nodes	Elements
Corner-ended configuration	9051	8699
Curve-ended with deflector configuration	9127	8752
Corner-ended with deflector configuration	9094	8718
Curved-ended configuration	8979	8635

Mass transfer analysis for the best chamber configuration

A multi-phase model was chosen in the ANSYS software, from which two-phases were selected. The first phase was renamed air, while the second phase representing shiitake mushrooms, was renamed water. Energy equation and RNG were enabled in the k-ε model and enhanced wall treatment. Respective boundary conditions were entered appropriately, as given in tab. 2. The water phase was assigned as the inlet with a mass fraction of 1.00 same as that of air. The solution was initialized using a standard scheme by inputting velocities and temperatures appropriately. The time interval was chosen as 0.1 second, and 2000 iterations were done. Calculations were done, and appropriate contours were generated.

Verifying the model in the twin cabinet dryer and drying experimentation

The model was verified by measuring velocity and temperature variation in the air inlet and dyer outlet, (numbered points in fig. 2, using a hot wire anemometer, AM20 model of Lutron Company, Taiwan. Model velocity and temperature discrepancies were compared with the experimental data. Then, approximately 250 kilograms of mushrooms were dried per trial using the best dryer configuration and drying conditions obtained. The average initial moisture content of mushrooms was 90.26% (wb). Drying continued until insignificant mass change was

observed in the real weight-measuring balance attached to the control panel. Moisture evaporated was determined:

$$m_w = \frac{m_i\left(x_i - x_f\right)}{100 - x_f} \quad \text{with} \quad m_f = m_i - m_w \tag{12}$$

Determination of lentinant content and rehydration ratio

Dried shiitake mushrooms at temperatures of 40 °C, 50 °C, 55 °C, and 60 °C were sampled into 500 g, coded and taken to Koking (Shanghai) testing service Co. The LTD for lentinan content determination at respective temperatures. Conversely, the rehydration ratio denotes the degree of mutilation caused by physical-chemical processes during most foods' drying processes [15]. An average of 20 g of mushrooms were dipped in a tap water flask for 30 minutes at room temperature. The wetted samples were then removed and dried off using tissue paper before being reweighed in an electronic balance. Rehydration ratio of mushrooms at varying temperatures:

$$R_h = \frac{W_r}{W_d} \tag{13}$$

Results and discussion

Drying air-flow distributions for the selected twin cabinet drying chamber configurations

Simulated velocity and temperature distribution using ANSYS FLUENT for four designs were done to determine the best twin-cabinet drying chamber configuration for drying shiitake mushrooms. Simulated velocities at a constant drying temperature of 40 °C for the selected twin cabinet drying chamber configurations are shown in fig. 3. It is observed that corner-ended with deflector configuration had the highest simulated velocity. For instance, Cabinet A had the highest velocity for the corner with deflector configuration followed by Cabinet A curved with deflector. Then curved with a deflector (Cabinet B), corner with deflector (Cabinet B), curved (Cabinet A), corner (Cabinet B), and curved (Cabinet B) followed each other, respectively, fig. 3(a). The same trend was observed when velocity was raised from 2-4 m/s and 6 m/s, figs. 3(b) and 4(c).

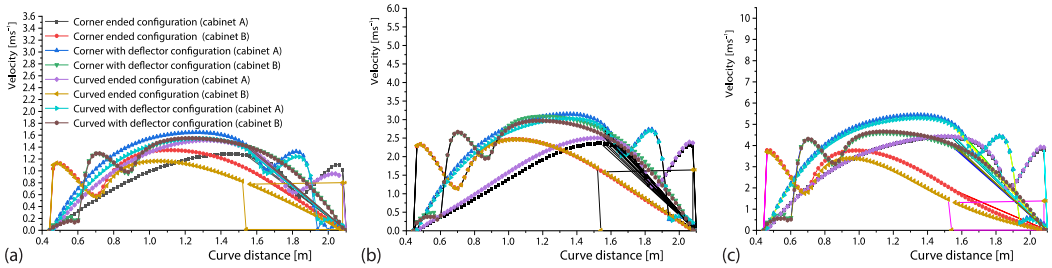

Figure 3. Simulated velocities at a constant drying temperature of 40 °C; (a) drying air input velocity of 2 m/s, (b) drying air input velocity of 4 m/s, and (c) drying air input velocity of 6 m/s

Simulating drying air velocities at 50 °C, fig. 4(a), corner with deflector (Cabinet A) had the highest velocity followed by curved with deflector (Cabinet A), curved with deflector (Cabinet B), corner with deflector (Cabinet B), curved (Cabinet A), corner (Cabinet B), corner (Cabinet A) and curved (Cabinet B). However, at 4 m/s, corner with deflector (Cabinet A) was

followed by corner with deflector (Cabinet B), curved with deflector (Cabinet A), curved with deflector (Cabinet B), corner (Cabinet B), curved (Cabinet B), curved (Cabinet A), and corner (Cabinet A), respectively, fig. 4(b). Simulating the drying velocity of 6 m/s, fig. 4(c), the corner with deflector (Cabinet A) was followed by curved with deflector (Cabinet A), curved with deflector (Cabinet B), corner with deflector (Cabinet B), curved (Cabinet A), corner (Cabinet A), corner (Cabinet B), and curved (Cabinet B).

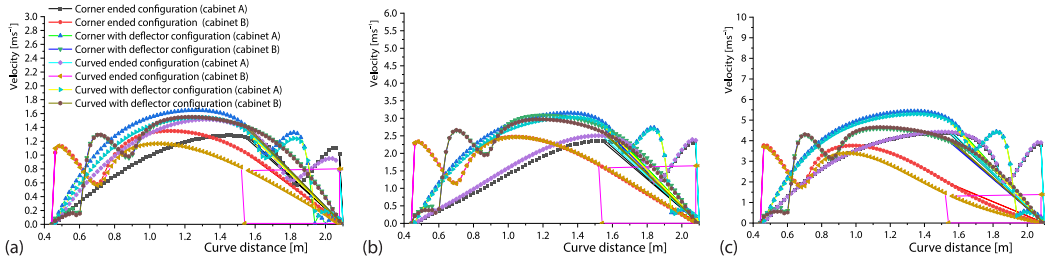

Figure 4. Simulated velocities at a constant drying temperature of 50 °C; (a) input velocity of 2 m/s, (b) input velocity of 4 m/s, and (c) input velocity of 6 m/s

Fixing temperature at 60 °C and velocity of 2 m/s, corner with deflector (Cabinet A) had the highest velocity followed by curved with deflector (Cabinet A), curved with deflector (cabinet B), corner with deflector (Cabinet B), curved (Cabinet A), corner (Cabinet B), corner (Cabinet A) and curved (Cabinet B). This observation was similar to those of fig. 4(a) at 50 °C constant temperature. Contrary, simulating at velocities of 4 m/s and 6 m/s showed similar trend with corner with deflector (Cabinet A) followed by corner with deflector (Cabinet B), curved with deflector (Cabinet A), curved with deflector (Cabinet B), corner (Cabinet B), curved (Cabinet B), curved (Cabinet A), and corner (Cabinet A), respectively, figs. 5(b) and 5(c). Therefore, it was adduced that adding deflector in the twin cabinet dryer helped reduce loss of velocity, improving distribution uniformity. The increase in air velocity with the employment of deflectors agrees with the findings of Roustapour *et al*. [16]. This implies that adding deflectors could increase the drying rate of the food. Additionally, curving the corners did not significantly impact air distribution since corner-ended and curved-ended trends showed sameness in velocity loss. Thus, deflectors improved drying air distribution in the twin cabinet dryers by deflecting drying air into the drying chamber, causing high value readings in air velocity due to forming a vortex and reduced direct exit when deflectors are unapplied. Air distribution was poor in the corner-ended configuration because there was an immediate exit of drying air at the far end, which was less resistant.

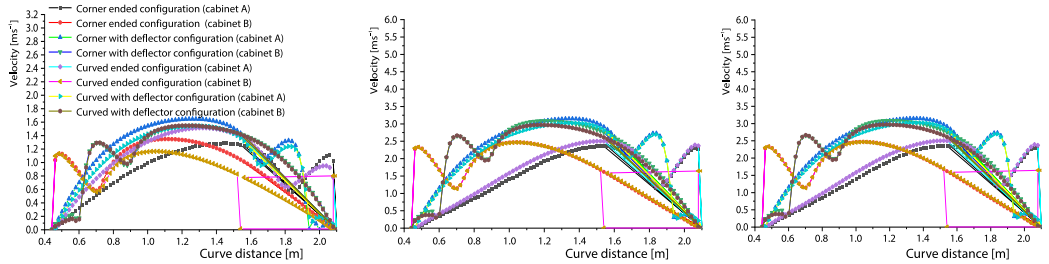

Figure 5. Simulated velocities at a constant drying temperature of 60 °C; (a) input velocity of 2 m/s, (b) input velocity of 4 m/s, and (c) input velocity of 6 m/s

Since uniformity and reduction in air velocity losses implied the most feasible dryer [5, 8], the corner-ended with deflector configuration was the best among the four configurations investigated. Therefore, configurations with deflectors would have high drying rates with the corner-ended deflector design leading. This was because installing deflectors increased residence time of drying air, leading to more moisture transfer from the intermolecular air spaces into the boundary zones for evaporation. This agreed with the findings of Nagle *et al*. [17]. Similar conclusions were observed in the numerical modelling of cabinets designed for melon drying using deflectors [18]. Configurations without deflectors had less drying capacity because the drying air tended to follow an unresistant path hence exiting with minimal utilization.

Figure 6 shows velocity distribution contours for corner-ended with deflector drying chamber design at 2 m/s, 4 m/s, and 6 m/s set velocities.

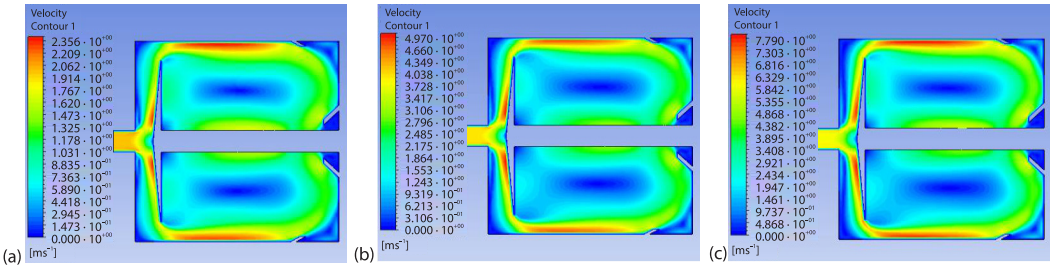

Figure 6. Velocity distribution profile for corner-ended with deflector dryer configuration; (a) velocity distribution at 2 m/s, (b) velocity distribution at 4 m/s, and (c) velocity distribution at 6 ms

As expected, air velocities are higher at the air inlet cavities and tended to follow an unresistant cavity to the far end from where it was bounced back into the drying area by deflectors. Again, there is a small region in each case with reduced velocity due to the vortex created by the swirling air-flow in the chamber that might cause low drying rates [2].

Temperature distributions for selected twin cabinet drying chamber configurations

The simulated temperatures for the selected heat pump twin cabinet dryer configurations are shown in figs. 7-9. At a constant velocity of 2 m/s and 40 °C, it was observed that there was a little non-uniform deviation in temperatures between Cabinets A and B for the curved configuration. There were minimum deviations between cabinets A and B for the corner-ended with deflector configuration. Corner-ended with deflector temperature deviations was slightly higher than other configurations except for Cabinet A of curved configuration with wide non-uniform temperature deviations with Cabinet B. A similar trend was true for simulations at 50 °C and 60 °C, figs. 7(a)-7(c).

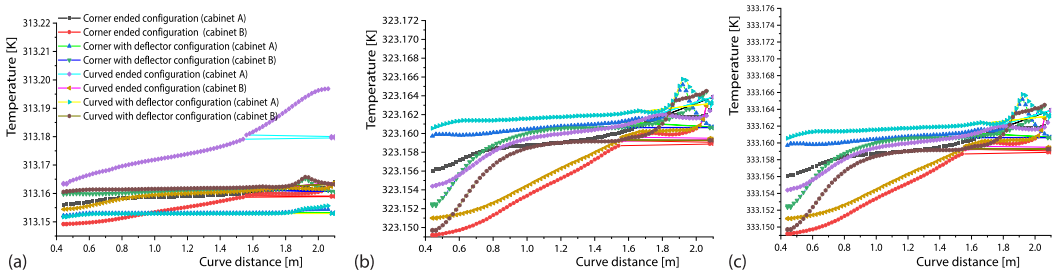

Figure 7. Simulated dryer temperature at a constant velocity of 2 m/s; (a) input temperature of 40 °C, (b) input temperature of 50 °C, and (c) input temperature of 60 °C

When velocities of 4 m/s at 40 °C were applied, temperature deviations in cabinets A and B were high and non-uniform for the curved and corner-ended configuration. There were uniform temperature deviations for Cabinets A and B of the corner with deflector configuration. This was similar to the curved with deflector configuration, fig. 8(a). However, at 50 °C and 60 °C, there was non-uniform temperature deviation between Cabinets A and B, but the margin reduced after the 1.0 m curved distance for the corner with deflector design. All the remaining configurations did not reduce or maintain a constant deviation, figs. 8(b) and 8(c). This implied non-uniformity in the quality of dried products.

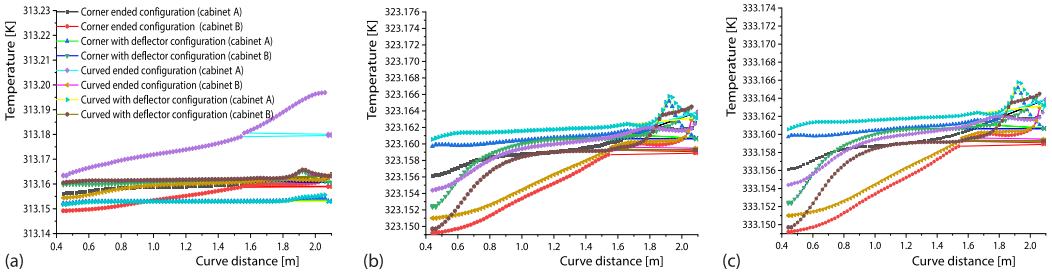

Figure 8. Simulated dryer temperature at a constant velocity of 4 m/s; (a) input temperature of 40 °C, (b) input temperature of 50 °C, and (c) input temperature of 60 °C

At 6 m/s and 40 °C, there were initial non-uniform temperature deviations, but the margin stabilized after the 1.0 m curve distance for Cabinets A and B in the corner with deflector configuration. A similar trend was observed at 60 °C for the curved with deflector design, though with slightly lower temperatures, fig. 9. For the remaining designs, there were non-uniform temperature margins. The observations indicate that adding deflectors helped diffuse hot air into the drying chamber better than when configurations had no deflectors.

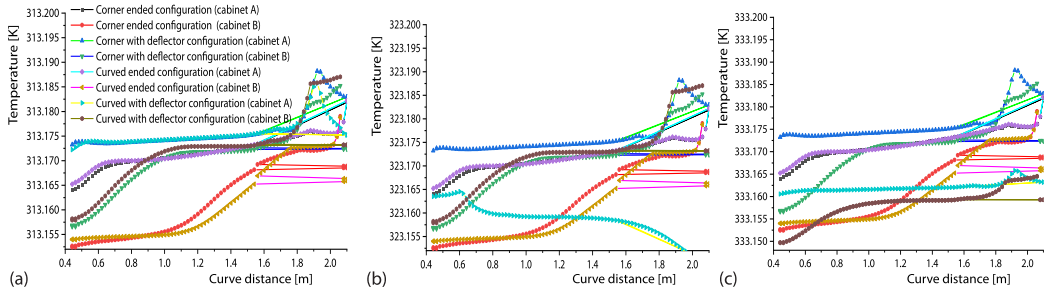

Figure 9. Simulated dryer temperature at a constant velocity of 6 m/s; (a) input temperature of 40 °C, (b) input temperature of 50 °C, and (c) input temperature of 60 °C

Consequently, the diverted air caused high temperature readings hence high drying rates, as reported by [16]. Configurations without deflectors had less drying capacity because the air followed a less impervious path and exited unutilized. Accordingly, corner-ended with deflector configuration was the most optimal configuration for the proposed twin cabinet dryer. Figure 10 shows temperature distribution contours for corner-ended with deflector design at temperatures of 40 °C, 50 °C, and 60 °C. The temperature distribution is slightly higher at the inlet to cavities than in the drying area. A keener look at the two drying chambers shows that cabinet A has better uniformity and higher temperature than Cabinet B. This was probably

caused by the renormalization grouping k-ε model used. However, the temperature variations caused were acceptable due to the small variations.

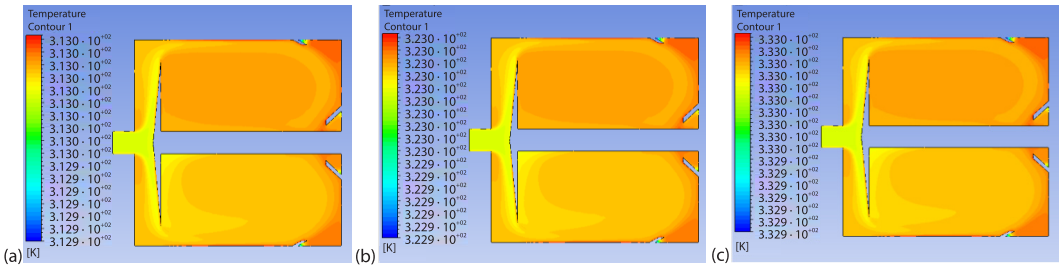

Figure 10. Temperature profiles for corner-ended with deflector configuration; (a) temperature distribution at 40 °C, (b) temperature distribution at 50 °C, and (c) temperature distribution at 60 °C

Comparison and selection of superior twin cabinet dryer configuration

Table 4 displays the configurations, temperature, and velocity combinations with the corresponding coefficient of determination, R^2). The R^2 was chosen to show how well-simulated data in Cabinet A data mapped in Cabinet B data. The high value of R^2 indicated good similarity and increased uniformity of parameter distribution between the two cabinets. Table 4 demonstrates that corner-ended with deflector configuration maintained better uniformity of above 84% in all the parameters simulated than the other configurations.

Mass transfer analysis for the optimised drying parameters of twin cabinet dryer

Figures 11(a) and 11(b) show contours for the vapor and air volume fraction of drying air for the twin heat pump cabinet dryer. The results reveal that moisture evaporations from mushrooms were higher at the corner-ended with deflectors and reduced from 100-11% in 2000 seconds. Figure 11(a), for instance, the fraction of water was lower in the drying area, inferring that the drying rate was high. Figure 11(b) agrees with fig. 12(a) because the air fraction was highest in the drying area, thus enabling an increased drying rate.

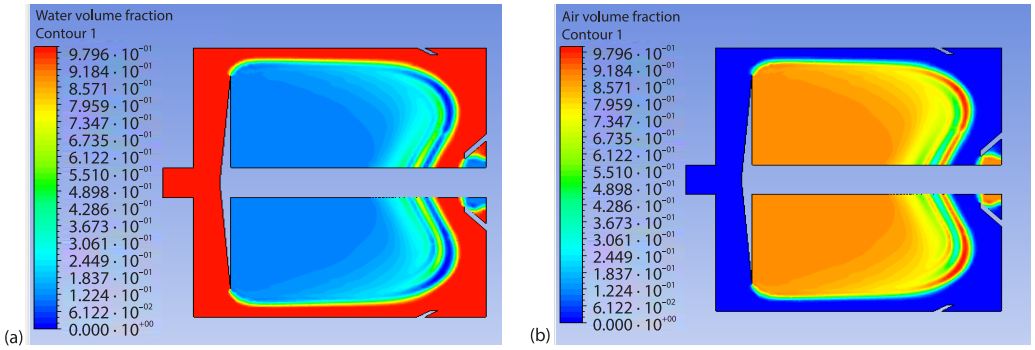

Figure 11. Vapour and air volume fraction of drying air for the twin cabinet dryer; (a) the vapor volume fraction of drying air and (b) the air volume fraction of drying air

A comparison of moisture removed from drying mushrooms in the two dryers is shown in fig. 12. Moisture removed showed a constant trend in both dryers between 2-18 hours of the experiment. However, after 18 hours of drying, the difference dropped due to the mois-

Table 4. Comparisons of air velocity and temperature distribution R^2 in the twin dryers

Configuration	Velocity [ms^{-1}]	Temperature [°C]	R^2	Configuration	Velocity [ms^{-1}]	Temperature [°C]	R^2
Corner-ended configuration	2	40	0.1248	Curve-ended configuration	2	40	0.1526
		50	0.1248			50	0.1526
		60	0.1248			60	0.1526
	4	40	0.0025		4	40	0.0009
		50	0.0025			50	0.0009
		60	0.0025			60	0.0009
	6	40	0.0028		6	40	0.0164
		50	0.0028			50	0.0164
		60	0.0028			60	0.0164
Corner-ended with deflector	2	40	**0.8343**	Curve-ended with deflector	2	40	0.8588
		50	**0.8343**			50	0.8588
		60	**0.8343**			60	0.8588
	4	40	**0.8413**		4	40	0.8081
		50	**0.8413**			50	0.8081
		60	**0.8413**			60	0.8081
	6	40	**0.8424**		6	40	0.8402
		50	**0.8424**			50	0.8402
		60	**0.8424**			60	0.8402

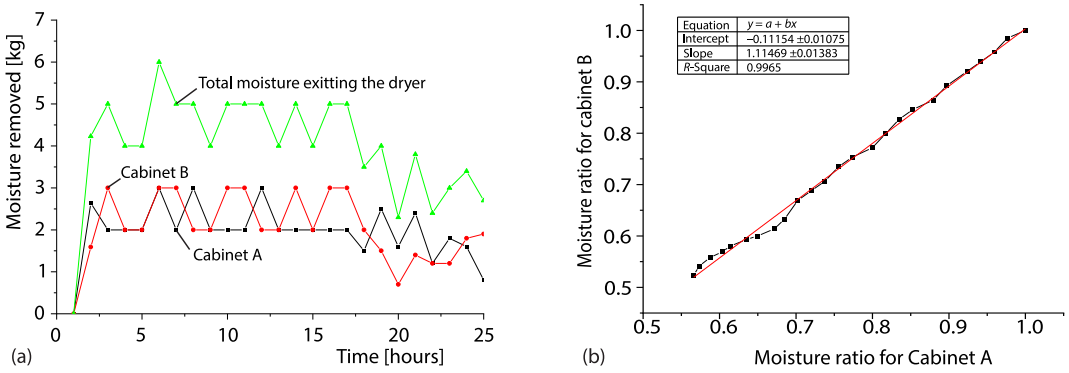

Figure 12. Comparisons of moisture ratios in the heat pump twin-cabinet dryer; (a) moisture removed comparisons and (b) comparisons between the two cabinets

ture depletion in the mushrooms. Slight usage of different masses (Cabinet A had 127.65 while Cabinet B had 123.32) caused slight variations, especially towards the end of drying.

Thus, comparing the moisture ratios in the two dryers showed that both moisture ratios mapped on each other well at $R^2 = 0.9965$, which is acceptable. As expected, the slight deviations of R^2 were due to variations in masses used in the two dryers and uncontrollable system design variations.

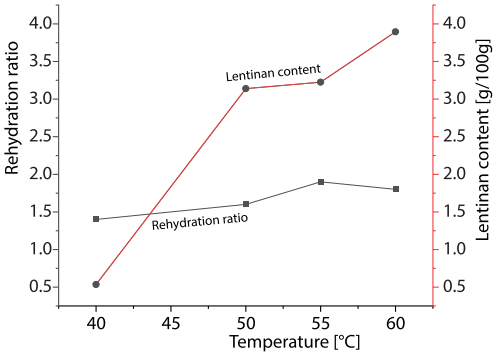

Figure 13. Influence of temperature on lentinan content and rehydration ratio of mushrooms

Impact of temperature variations on Lentinan content and rehydration ratio

Figure 13 is a graphical representation of the impacts of temperature variation on lentinan content and rehydration ratio of shiitake mushrooms. These results were obtained after drying 500 g of shiitake mushrooms at temperatures of 40 °C, 50 °C, 55 °C, and 60 °C to determine the best temperature with an acceptable quality of dried mushrooms. For instance, Lentinans are vital to the body because the immune system recognizes them and encourages adaptive and innate immune responses [19]. The rehydration ratio on dried food products is used as a leader in structural quality that depends on the drying processes applied [20]. Figure 13 shows that lentinan content increased with a rise in temperature from 40-60 °C. This was attributed to the fact that water, which took the bulky mass, was removed, leaving the lentinan content high in terms of dry basis. This improved the quality of the dried shiitake mushroom. The rehydration ratio, fig. 13, also increased with temperature increase.

The high temperature increased moisture transfer from the mushrooms, and thus rehydration would also increase due to the creation of intermolecular pores that caused more water reabsorption. This phenomenon caused high rehydration. Other researchers have reported this phenomenon, especially on shiitake mushrooms [21]. Since high lentinan content and rehydration ratio are preferred in most dried food, drying shiitake mushrooms at 55-60 °C was considered optimal. High temperatures reduce drying time with high lentinan content and rehydration ratio, as reported in other researches [22, 23].

Conclusion

Employing proper drying configuration helps ensure uniform heat and mass transfer processes. This paper investigated four heat pump twin cabinet dryer designs concerning temperature and velocity distribution uniformity, with the superior design being fabricated. Drying temperature and velocity distribution patterns were analyzed using CFD techniques to determine the best design before fabrication. It was found that adding deflectors to the main air stream helped improve air distribution and temperature distribution in the dryers compared to those without deflectors. Curving the corners had an insignificant effect on parametric distribution trends. Corner-ended with deflectors configuration at the specified angles proved superior among the investigated designs. A 6 m/s velocity and 60 °C temperature had the least deviations concerning the simulated values (R^2 = 0.8424). Simulation for mass transfer of the corner-ended with deflectors configuration using the optimal conditions caused a vapor reduction from 1.00-0.11 in 2000 seconds. An experimental moisture ratio correlation in the two dryers was R^2 = 0.9965 which is acceptable. A temperature of 55-60 °C gave better lentinan content and rehydration ratio.

Acknowledgment

The research has been supported by the Jiangsu Special Fund for Innovation and Extension of Agricultural Science and Technology (Project No. NJ2019-15).

Nomenclature

$C_{1\varepsilon}$, $C_{2\varepsilon}$, $C_{3\varepsilon}$, – constants used in turbulent model
C_p – specific heat capacity at constant pressure
c_a – specific heat capacity of drying air, [kJkg^{-1}K^{-1}]
c_g – specific heat capacity of vapour, [kJkg^{-1}K]
c_w – specific heat capacity of water, [kJkg^{-1}K^{-1}]
D_{eff} – effective diffusivity
E – total energy, [kJ]
G_b – generation of turbulent kinetic energy due to buoyancy
G_k – generation of turbulent kinetic energy due to the mean velocity gradients
h_s – heat sorption of water in mushrooms
k – turbulent kinetic energy, [m^{2}s^{-2}]
k_{eff} – mushrooms' effective thermal conductivity, [Wm^{-1}K^{-1}]
m_f – dry matter of product, [kg]
m_i – initial matter of product, [kg]
m_w – evaporated water, [kg]
Pr – Prandtl number
p – pressure
R_h – rehydration ratio
S_i – source term for ith momentum equation
S_k, S_ε, S_w, S_h – user-defined source terms
T – temperature, [K]
∂T – temperature change, [K]
∂t – change in time
t – time, [second]
Δt – change in time, [second]
u – velocity magnitude in x-direction, [ms^{-1}]
V_{xy} – mass transfer coefficient
W – moisture content of mushrooms, [kg/kg dry air]
W_e – equilibrium moisture content of mushrooms, [kg water/kg dry air]
W_d – mass of dried mushrooms, [kg]
W_n – moisture content of mushrooms after nth time step, [kg water/kg dry air]
W_{n+1} – subsequent moisture content of mushrooms after nth time step, [kg water/kg dry air]
W_r – rehydrated mushrooms' mass, [kg]
∂w – mass change
x_i – initial moisture content of mushrooms, (d.b.)
x_f – final moisture content of mushrooms, (d.b.)
Y_m – contribution of the fluctuating dilatation in compressible turbulence to dissipation rate

Greek symbols

ε – dissipation rate, [m^{2}s^{-3}]
μ – dynamic viscosity
μ_t – turbulent viscosity
ρ – fluid density
ρ_a – drying air density, [kgm^{-3}]
ρ_b – bulk density
ρ_m – wet mushroom density
ρ_s – particle density of mushrooms, [kgm^{-3}]
σ_k – turbulent Prandtl numbers for k
σ_ε – turbulent Prandtl numbers for ε
$(\tau_{ij})_{\text{eff}}$ – deviatoric stress tensor
∇ – rate of change in special co-ordinate, [m^{-1}]
ϑ_i – velocity vector in x-direction
ϑ_j – velocity vector in y-direction
ϑ_{mag} – velocity magnitude

References

[1] Purusothaman, M., *et al*. The CFD Analysis of Greenhouse Solar Dryer with Different Roof Shapes, *Proceedings*, 5th International Conference on Science Technology Engineering and Mathematics (ICONSTEM), Sathyabama Institute of Science and Technology: IEEE, Chennai, India, 2019
[2] Natalia, S. V., *et al*., Drying uniformity Analysis in a Tray Dryer, An Experimental and Simulation Approach, *Advance Journal of Food Science Technology*, *15* (2018), S, pp. 233-238
[3] Darabi, H., *et al*., Design a Cabinet Dryer with Two Geometric Configurations Using CFD, *Journal of Food Science Technology*, *52* (2013), 1, pp. 359-366
[4] Carrera, E. J. L., *et al*., Computational Fluid Dynamics Analysis for Improving Temperature Distribution in a Chili Dryer, *Thermal Sciences*, *2*2 (2018), 6A, pp. 2615-2623
[5] Babu, A., *et al*., The CFD Studies on Different Configurations of Drying Chamber for Thin-Layer Drying of Leaves, *Energy Sources*, *42* (2020), 18, pp. 2227-2239
[6] Norton, T., *et al*., Computational Fluid Dynamics in the Design and Analysis of Thermal Processes: A Review of Recent Advances, *Critical Reviews in Food Science Nutrition*, *53* (2013), 3, pp. 251-275
[7] Ozcan-Coban, S., *et al.*, A Review on Computational Fluid Dynamics Simulation Methods for Different Convective Drying Applications, *Thermal Sciences*, *27* (2023), 1B, pp. 825-842
[8] Carlescu, P. M., *et al*., The CFD Simulation of Heat and Mass Transfer during Apricots Drying, *LWT-Food Science Technology*, *85* (2017), 85, pp. 479-486
[9] Singh, R., *et al*., The CFD Modelling and Simulation of an Indirect Forced Convection Solar Dryer, in: *IOP Conference Series, Earth and Environmental Science*, IOP Publishing, Bristol, UK, 2021
[10] Pal, U., *et al*., Calculation Steps for the Design of Different Components of Heat Pump Dryers under Constant Drying Rate Condition, *Drying Technology*, *26* (2008), 7, pp. 864-872

[11] Singh, R. P., *et al.*, *Introduction Food Engineering*, 4th ed., Gulf Professional Publishing, Houston, Tex., USA, 2001
[12] Muralikrishna Sharma, I. V. N., *et al*., Numerical Simulation of a New Optimized Cabinet Dryer for Apple Drying, *International Journal of Mechanical and Production Engineering Research and Development (IJMPERD*), *10* (2020), 4, pp. 59-72
[13] Yongson, O., *et a*l., Air-Flow Analysis in an Air Conditioning Room, *Building Environment*, *42* (2007), 3, pp. 1531-1537
[14] Rhim, J. W., *et al*., Drying Kinetics of Whole and Sliced Shiitake Mushrooms (*Lentinus edodes*), *Food Science Biotechnology*, *20* (2011), 2, pp. 419-427
[15] Doymaz, I., Drying Kinetics and Rehydration Characteristics of Convective Hot-Air Dried white Button Mushroom Slices, *Journal of Chemistry*, *2014* (2014), ID453175
[16] Roustapour, O. R., *et al*., Numerical modelling of Air-Flow in a Cabinet Dryer Equipped by Deflector Plates, *International Journal of Food Engineering*, *15* (2019), 10
[17] Nagle, M., *et a*l., Effects of Operating Practices on Performance of a Fixed-Bed Convection Dryer and Quality of Dried Longan, *International Journal of Food Science Technology*, *43* (2008), 11, pp. 1979-1987
[18] Omid, R. R., *et al*., Numerical Modelling of Air-Flow in a Cabinet Dryer Equipped by Deflector Plates, *International Journal of Food Engineering*, *15* (2019), 10, pp. 1-11
[19] Sari, M., *et al.*, Screening of Beta-Glucan Contents in Commercially Cultivated and Wild Growing Mushrooms, *Food Chemistry*, *216* (2017), Feb., pp. 45-51
[20] Kantrong, H., *et al*., Drying Characteristics and Quality of Shiitake Mushroom Undergoing Microwave-Vacuum Drying and Microwave-Vacuum Combined with Infrared Drying, *Journal of Food Science and Technology*, *12* (2014) 51(12), pp. 3594-3608
[21] Subramaniam, S., *et al*., Changes in the Morphometric, Textural, and Aromatic Characteristics of Shiitake Mushrooms during Combined Humid-Convective Drying, *Drying Technology*, *39* (2021), 16, pp. 2206-2217
[22] Kantrong, H., *et al.*, Drying Characteristics and Quality of Shiitake Mushroom Undergoing Microwave-Vacuum Drying and Microwave-Vacuum Combined with Infrared Drying, *Journal of food science Technology*, *51* (2014), 12, pp. 3594-3608
[23] Timm, T. G., *et al*., Drying Process of *Lentinula edodes*: Influence of Temperature on β-Glucan Content and Adjustment Of Mathematical Models, Ciência e Agrotecnologia, *43* (2020), 2-3, pp. 1-12

Paper submitted: March 5, 2023
Paper revised: April 15, 2023
Paper accepted: April 24, 2023